THE ANALYST
FULL PAPER
www.rsc.org/analyst

Carbon nanotube-modified electrodes for the simultaneous determination of dopamine and ascorbic acid

Zonghua Wang,[ab] Jun Liu,[a] Qionglin Liang,[a] Yiming Wang[a] and Guoan Luo*[a]

[a] *Department of Chemistry, Tsinghua University, Beijing 100084, China. E-mail: galuo@chem.tsinghua.edu.cn*
[b] *Department of Chemistry, Qingdao University, Qingdao 266071, China*

Received 29th January 2002, Accepted 12th March 2002
First published as an Advance Article on the web 18th April 2002

The voltammetric separation of dopamine and ascorbic acid was studied with cyclic voltammetry at two kinds of carbon nanotube-modified electrodes (coated and intercalated). The anodic peak difference reached 270 mV under the present conditions. The separation mechanism and effect factors were carefully studied. Using various types of surfactants as coating dispersants of carbon nanotubes, it was demonstrated that the charge nature of the surfactants had a strong effect on the electrochemical behavior of dopamine and ascorbic acid. When the oxidation solution of carbon nanotubes was changed from the most commonly used mixed concentrated nitric acid and sulfuric acid (1 + 3 v/v) to dilute nitric acid and to hydrochloric acid, the anodic peak separation value of dopamine and ascorbic acid increased significantly, and it was shown that carboxylic acid groups attached to the carbon nanotubes were an adverse factor for the discrimination of DA from AA. These results indicated that the resolution of DA and AA was mainly attributable to the stereo porous interfacial layer formed from aggregated pores and inner cavities of the carbon nanotubes. The modified electrodes exhibited an attractive ability to measure DA and AA simultaneously and showed good stability and reproducibility.

Introduction

Carbon nanotubes (CNT) constitute a new structure of graphitic carbon consisting of one or several concentric tubules each with a helically wound hexagonal honeycomb lattice, and can be divided into multi-wall carbon nanotubes (MWNT)[1] and single-wall carbon nanotubes (SWNT)[2] according to the carbon atom layers in the wall of the nanotubes. CNT have an aspect ratio ranging from 100 to 1000. Interest in CNT stems from their unique geometric, mechanical, electronic and chemical properties. The one-dimensional tubular structure of CNT extends the research field of nanomaterials, and intense interest is now being focused on the wide potential applications when various methods of synthesizing CNT have been developed.[3,4]

Using nanomaterials to modify electrodes, in addition to the common effects of the inherent physical and chemical properties that are introduced, special properties such as the large specific surface area and the abundant functional groups help them to show specific catalytic action in the electrochemical reactions of certain substances.[5–7] Depending on their atomic structure, CNT behave electrically as a metal or as a semiconductor. The subtle electronic properties suggest that CNT have the ability to promote electron-transfer reactions when used as an electrode in chemical reactions. It has been reported that a microelectrode was constructed from individual SWNT and its voltammetric response was characteristic of steady-state radial diffusion.[8] An electrode constructed from MWNT mixed with bromoform can be used to catalyze the oxidation of dopamine (DA)[9] and showed a favorable reversible electrochemical response to cytochrome *c* and azurin.[10] The activity of enzymes can be stabilized well using CNT immobilization.[11] A cast film of SWNT on Pt and Au electrodes has been reported,[12] but it did not show well-resolved voltammograms. A carboxylic SWNT solution was cast on a glassy carbon electrode to form a carbon nanotube film, which showed very stable electrochemical behavior and can be used to catalyze the electrochemical reactions of some biomolecules such as dopamine, epinephrine, ascorbic acid (AA)[13,14] and 3,4-dihydroxyphenylacetic acid.[15] DA and AA, however, have similar anodic peak potentials (E^{DA}_{pa} = 0.182 V, E^{AA}_{pa} = 0.16 V).[14] No other papers seem to have reported on the application of CNT for the voltammetric separation of DA from AA, and this prompted us to investigate the selectivity of DA in the presence of AA in this work.

DA is one of the most significant catecholamines and belongs to the family of excitatory chemical neurotransmitters.[16] The electrochemical determination of DA, however, was restricted in an excess of AA, which has a similar oxidation potential to DA. Bioelectrochemists and electroanalytical chemists have been showing great interest in this area and various modified electrodes have been constructed for this purpose.[17–26] Because of the simple preparation and easy refreshing of the surface, carbon has been used extensively as a working electrode for a variety of electrochemical applications. It has also been shown that carbon tends to be more compatible with biological tissues than other commonly used electrode materials.[16] The current routes to improving the selectivity of carbon electrodes include pre-treatment and modifications of the electrode surface such as laser activation,[27] heat treatment,[28] electrochemical pre-anodization,[29] various permselective membranes,[30,31] polymer films[19,32] and even the introduction of new carbon electrode materials [*e.g.*, graphite reinforced with carbon (GRC)].[33] As a new type of carbon nanomaterial, CNT have porous structure and large specific surface area. Furthermore, the matrix of brain tissue shows no inhibition of DA oxidation or dopaminequinone reduction when using CNT as a working electrode.[9] On the other hand, CNT with a nanometer-order diameter and micrometer-order length or longer[4] are suitable to implement miniaturization of the electrode.[8] Despite the advantages mentioned above, enhancement of the selectivity of CNT electrodes is crucial for practical applications. In this work, two kinds of CNT-modified electrodes (coated and intercalated) were constructed. The effects of dispersant and the intrinsic properties of CNT on the discrimination of DA from AA were investigated. The modified electrodes exhibited an attractive ability to separate DA and AA effectively and showed good

stability and reproducibility. These favorable features indicate great promise for *in vitro* and *in vivo* applications of carbon nanotube-modified electrodes.

Experimental

Apparatus

Cyclic and differential pulse voltammetric (CV and DPV) experiments were performed using a CHI-660 electrochemical workstation (CH, USA) with a conventional three-electrode cell. The working electrode was a graphite electrode or CNT-modified graphite electrode with an electrode area of 19.62 mm^2, the auxiliary electrode consisted of a platinum wire and the reference electrode was a saturated calomel electrode (SCE). All the potentials given in this paper are *versus* SCE. Scanning electron microscope (SEM) images were obtained using a thermal field emission scanning electron microscope (LEO 1530, Germany). Fourier transform (FT) IR spectra were recorded on a Perkin-Elmer Spectrum GX spectrometer.

Chemicals

All reagents were of analytical-reagent grade. Dopamine, ascorbic acid, Triton X-100, β-cyclodextrin (β-CD) and sodium dodecyl sulfate (SDS) were obtained from Sigma and hexadecyltrimethylammonium bromide (CTMAB) from Beijing Chemical Factory. High-purity nitrogen was used for deaeration. All solutions were prepared with doubly distilled water. Twist MWNT with an average external diameter of 40 nm were kindly provided by Dr. Wei Fei (Chemical Engineering Department of Tsinghua University, Beijing, China).

Pre-treatment of MWNT

In order to eliminate metal oxide catalysts, 0.2 g of MWNT were dispersed in 60 ml of 6.0 M HCl for 4 h with the aid of ultrasonic agitation, washed until the pH of the solution approached 7 and finally dried. An experimental specimen of >90% purity was obtained, denoted MWNT-1.

Oxidation of MWNT-1

A 0.05 g amount of MWNT-1 was dispersed in 60 ml of 2.2 M HNO_3 for 20 h at room temperature with the aid of ultrasonic agitation, then washed with distilled water to neutrality and dried. The sample obtained was denoted MWNT-1a. Another sample denoted MWNT-1b (functionalized with carboxylic acid groups[34–36]) was prepared following similar procedures, except that the dispersion solution was replaced with 80 ml of mixed concentrated HNO_3 and H_2SO_4 (1 + 3 v/v) and the time for ultrasonic agitation was 6 h.

Preparation of carbon nanotube-modified electrodes

A pyrolytic graphite electrode was carefully polished with emery paper and chamois leather containing an Al_2O_3 slurry (0.05 μm after 0.3 μm) and then ultrasonically cleaned in distilled water. A carbon nanotube-coated graphite electrode (CNT-CE-1) was prepared by dropping a solution of 1.5 mg of MWNT-1 specimen dispersed in 1 ml of dispersant on the graphite electrode surface and then heating under an IR lamp to remove the solvent. A carbon nanotube-intercalated graphite electrode (CNT-IE) was fabricated by grinding with asuitable amount of CNT powder. A thin CNT layer was formed on the graphite surface by intercalating the CNT into the soft graphite layers with the aid of mechanical force and also the action of chemical and physical adsorption. Prior to the electrochemical experiment, CNT-IE was washed in distilled water.

Procedures

All experiments were carried out at room temperature (~ 20 °C) under an atmosphere of nitrogen. CV employed a scan rate of 50 mV s^{-1}. DPV were performed with pulse potential 50 mV, pulse duration 50 ms and pulse period 0.2 s. A 50 mM NaH_2PO_4 solution (pH 5.0) was used as the supporting electrolyte.

Results and discussion

Physical characterization

The same stereo porous layer formed by twist MWNT with an average diameter of 40 nm can be observed at both CNT-IE-1 and CNT-CE-1 at high magnification (Fig. 1 shows the SEM image of CNT-IE-1). At low magnification (5 K, not shown), however, a smooth surface was visible except that some CNT was present around the interstices at CNT-IE-1, whereas a rugged surface was observed at CNT-CE-1.

Voltammetry of DA and AA at CNT-modified electrodes

The voltammetric behavior on a bare graphite electrode, CNT-CE-1 (water as solvent) and CNT-IE-1, was studied, and a comparison of the CV results is shown in Fig. 2. DA could not

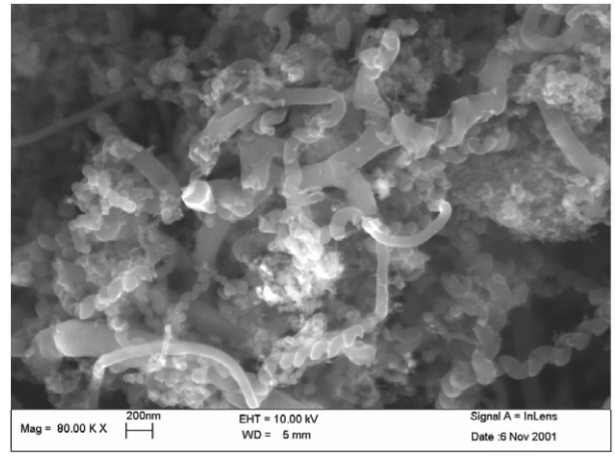

Fig. 1 SEM image of the twist MWNT-1 intercalated on a graphite disk. Magnification 80 000×.

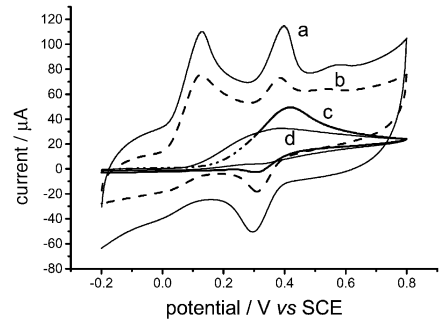

Fig. 2 Cyclic voltammograms of a mixture of 2×10^{-4} M DA + 1×10^{-3} M AA at (a) CNT-IE-1, (b) CNT-CE-1, (c) damaged CNT-coated electrode and (d) bare graphite electrode. Electrolyte: 50 mM NaH_2PO_4. Scan rate: 50 mV s^{-1}.

be discriminated from AA when a bare graphite electrode was used [Fig. 2(d)]. When CNT-IE-1 or CNT-CE-1 was used as the working electrode, the detection sensitivity was improved significantly and effective separation of the anodic peaks of DA and AA was obtained [Fig.2(a) and (b)]. Compared with the bare electrode, in addition to the fact that the stereo porous interfacial layer of CNT-modified electrodes with high specific surface area[37] increases the conductive area, DA and AA can penetrate through the conductive porous channel onto the electrode more easily, leading to higher sensitivity. The anodic peak potentials were the same when employing CNT-IE-1 and CNT-CE-1 (E^{DA}_{pa} = 0.40 V, E^{AA}_{pa} = 0.13 V, $\triangle E$ = 270 mV), but the sensitivity of the former was slightly higher. This was probably because the surface of the graphite was soft and, during grinding, some fresh surfaces were generated and oxygenic groups were carried.[38] The pores in aggregated MWNT can be mainly divided into inner hollow cavities of smaller diameter (narrowly distributed, mainly 3.0–4.0 nm) and aggregated pores (widely distributed, 20–40 nm), which were formed by the interaction of isolated MWNTs.[39] The different modification routes had little effected on the peak potentials of DA and AA, indicating that the similar porous microstructures at CNT-CE and CNT-IE (confirmed by SEM) led to analogous electrocatalytic behaviors. Further experiments were performed to confirm this speculation. When MWNT-1 was boiled in concentrated HNO_3 for a long period, the tubule structure was totally damaged (Fig. 3) and then discrimination of DA from AA could not be achieved [Fig. 2(c)]. It was further demonstrated that the tubular structure of CNT played a major role in the voltammetric separation of DA and AA. Compared with a bare electrode [Fig. 2(d)], the sensitivity was improved to some extent [Fig. 2(c)], which could be caused by the existence of oxygen-containing groups.

Dependence of voltammetric resolution of DA and AA at CNT-IE-1 on pH. With increasing pH (3–9), the peak potentials of both DA and AA were shifted to more negative values (not shown). This is a consequence of a deprotonation step involved in both oxidation processes that is facilitated at higher pH. The anodic peak potential difference ($\triangle E_{pa}$) decreased (the DPV results are given in Table 1) with increase in pH. The anodic peak current ratio of DA to AA (I^{DA}_{pa}/I^{AA}_{pa}) was maximum at pH 7 and this was advantaged for detecting DA at physiological pH. In this work, the discrimination mechanisms and simultaneous determination of DA and AA were mainly investigated, so 50 mM NaH_2PO_4 at pH 5.0 was chosen as the supporting electrolyte.

Effect of dispersant. To demonstrate how the charged nature of the interfacial layer affected the electrocatalytic behavior at CNT-CE, various kinds of surfactant (anionic, cationic, non-ionic) aqueous solutions (2% w/v) were used as dispersants. The DPV curves in Fig. 4 show clearly that this factor had a significant effect on the discrimination of DA from AA. Compared with pure water as the dispersant [Fig. 4(a)], when the anionic surfactant SDS [Fig. 4(d)] was added, the peak potential of DA (E^{DA}_{pa}) was not obviously affected, whereas that of anionic AA (E^{AA}_{pa}) distinctly shifted to more positive values, hence $\triangle E_{pa}$ decreased; further, from the same figure, it was observed that the ratio of current signals, I_{DA}/I_{AA}, increased. This could be explained by the negative charges of SDS being electrostatically repulsive to AA (the structure is shown in Fig. 5), which inhibited the oxidation of AA. A similar explanation can be applied to Fig.4(c). The cationic surfactant CTMAB shifted E^{DA}_{pa} to more positive values without changing E^{AA}_{pa}, and it also lowered the reversibility of the redox of DA (the structure is shown in Fig. 5) and decreased the value of I_{DA}/I_{AA}. The non-ionic surfactant Triton X-100 shifted the peak potentials of both DA and AA to more positive values [Fig. 4(e)]; this indicated that the non-polar and long-chain molecular structure had a negative effect on the redox of DA and AA. When β-CD was used as dispersant, the peak potential of AA also shifted positively [Fig. 4(b)], but the shift was less than that of SDS, because the negativity of the hydroxyl group (OH) belonging to β-CD was weaker than that of the anion ($C_{12}H_{25}O_4S^-$).

Effect of carbon nanotubes with acid treatment on voltammetric behavior. CNT-IE-1, CNT-IE-1a and CNT-IE-1b were constructed with MWNT-1, MWNT-1a and MWNT-1b, respectively. The CV curves and results are shown in Fig. 6 and Table 2. When CNT was oxidized with acids of increasing oxidizing capability, namely dilute HCl, HNO_3 and mixed concentrated HNO_3 and H_2SO_4 (1 + 3), the peak potential of DA shifted slightly, whereas that of AA shifted to more positive

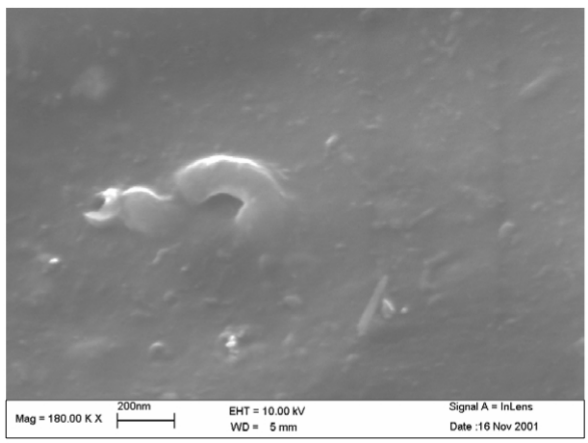

Fig. 3 SEM image of MWNT-1 damaged by the oxidation with concentrated HNO_3. Magnification 180 000×.

Table 1 Dependence of anodic potentials different of DA and AA on pH at CNT-IE-1 (1 mM DA + 1 mM AA). Conditions as in Fig. 2

	pH						
	3.0	4.0	5.0	6.0	7.0	8.0	9.0
$\triangle E_{pa}$/mV	280	275	270	250	220	200	175
I^{DA}_{pa}/I^{AA}_{pa}	3.60	3.87	6.73	8.52	16.26	10.27	7.23

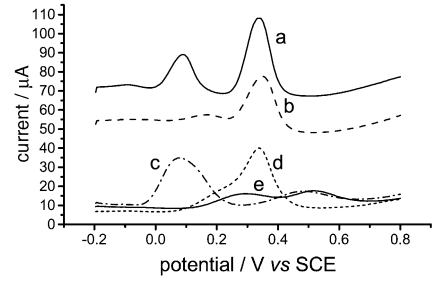

Fig. 4 DPVs of a mixture of 2×10^{-4} M DA + 1×10^{-3} M AA at CNT-CE-1 dispersed with different kinds of surfactants. (a) H_2O, (b) ß-CD, (c) CTMAB, (d) SDS and (e) Triton X-100. Electrolyte: 50 mM NaH_2PO_4. Scan rate: 50 mV s^{-1}.

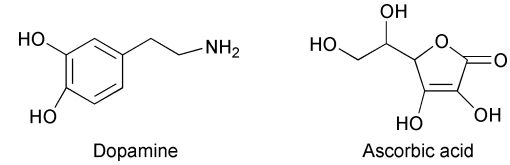

Fig. 5 Structures of dopamine and ascorbic acid.

values, with the result that the value of $\triangle E_{pa}$ decreased and I_{DA}/I_{AA} increased.

The end, pentagon, heptagon and curvature positions of carbon nanotubes are inclined to be oxidized to carboxyl, especially with more structural defects of MWNT. Therefore, an acid is favorable for oxidation and truncation of CNT. The length of CNT differed with the extent of oxidation. From the SEM image an obvious corrosive imprint can be observed on the carbon nanotube and the average length of the tubes decreased with increasing oxidation capability of the acid. Many short tubes (~ 200 nm) were visible after treatment with mixed concentrated acids (Fig. 7). In our opinion, CNT with various aspect ratios resulting from oxidation formed different stereo microstructures in the interfacial layers; on the other hand, the electronic properties of CNT might be changed due to acid treatment, which resulted in different electrocatalytic behaviors.

The nature of the surface groups was further investigated using FTIR spectroscopy (Fig. 8). The high absorbance of the nanotubes necessitated a very low sample concentration and therefore there is likely to be significant water contamination (corresponding to the signals at 1615–1632 cm^{-1}). It is generally also accepted that the interpretation of surface groups can only be qualitative, as they cannot be expected to behave as isolated functional groups.[40] Fig. 8 indicates the difference in absorbance for functionalized groups among the samples of MWNT: the peak at 1719 cm^{-1} is associated with C=O stretching of carboxylic acids, which occurred only at the MWNT-1b and MWNT-1a [Fig. 8(a) and (c)], with stronger absorbance for the former. The peak at 1056 cm^{-1}, corresponding to the C–OH stretch mode, was observed much more intensesly from the IR spectra of MWNT-1b than from the other two. This further proved that the stronger the oxidizing acid used, the more carboxylic and hydroxyl groups were introduced. The hydrophilic oxygen-rich groups introduced increased the negativity of MWNT, which enhanced the electrostatic repulsion towards AA and decelerated the oxidation reaction; therefore, the peak potential of AA shifted to more positive values with the increasing extent of oxidation of CNT. This effect was similar to that of ß-CD and SDS mentioned above.

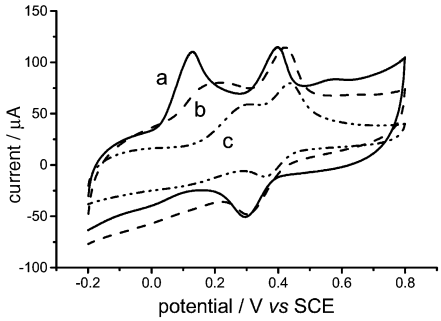

Fig. 6 CVs of a mixture of 2×10^{-4} M DA + 1×10^{-3} M AA at (a) CNT-IE-1, (b) CNT-IE-1a and (c) CNT-IE-1b. Electrolyte: 50 mM NaH_2PO_4. Scan rate: 50 mV s^{-1}.

Table 2 Effect of acid pre-treatment on voltammetric behavior at CNT-IE

Electrode	E^{DA}_{pa}/V	E^{AA}_{pa}/V	ΔE_{pa}/V	I_{DA}/I_{AA}
CNT-IE-1	0.398	0.129	0.269	0.69
CNT-IE-1a	0.422	0.191	0.231	1.42
CNT-IE-1b	0.437	0.278	0.159	1.51

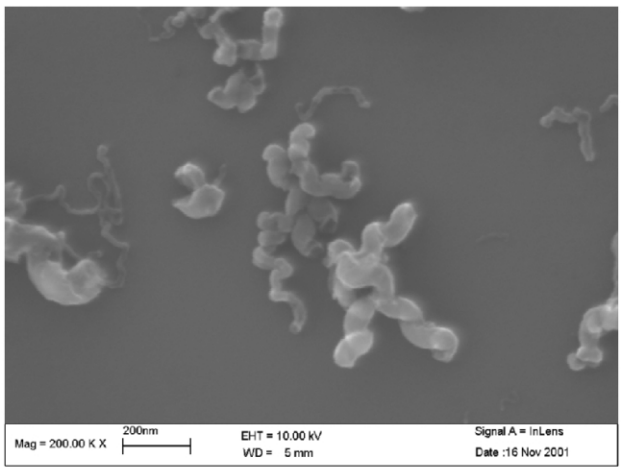

Fig. 7 SEM image of MWNT-1b. Magnification 200 000×.

Electrocatalysis of CNT-IE-1 towards DA and AA. Using CNT-IE-1 as the working electrode, the electrochemical behavior of redox of DA in 50 mM NaH_2PO_4 solution was studied employing CV [Fig. 9(b)]. Compared with the bare electrode [Fig. 9(d)], the peak current of DA was obviously increased and the reversibility improved (E_{pa} = 0.380 V, E_{pc} = 0.254 V). The tubular structure of the CNT effectively inhibited the cyclization and subsequent polymerization of DA, which improved the reversibility and enhanced the anticontaminative capability.[32] The peak current was proportional to the square root of the scan rate in the range 5–400 mV s^{-1}, which indicated that the mechanism of the electrode process was related to diffuse transmission. The CNT-IE-1 exhibited effective electrocatalysis towards AA [Fig. 9(a)], with the result that the peak current increased more than twofold and the peak potential shifted to 0.140 V with a spiky peak. The peak current was found to be linear with the square root of scan rate in the range 5–400 mV s^{-1}. This indicated that the electrode reaction was controlled by diffusion processes.

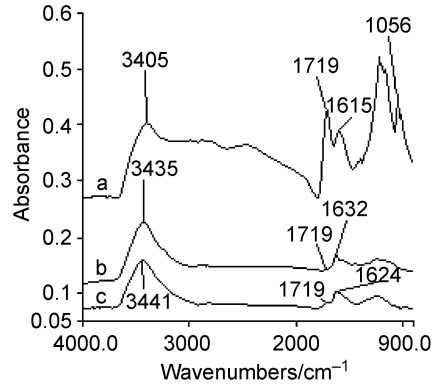

Fig. 8 IR spectra of (a) MWNT-1b, (b) MWNT-1 and (c) MWNT-1a.

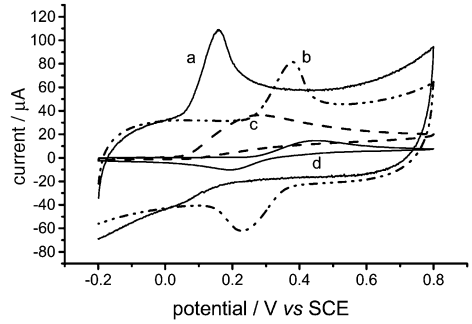

Fig. 9 CV recordings of 1×10^{-3} M AA at (a) CNT-IE-1 and (c) bare graphite electrode and 2×10^{-4} M DA at (b) CNT-IE-1 and (d) bare graphite electrode. Electrolyte: 50 mM NaH_2PO_4. Scan rate: 50 mV s^{-1}.

Analytical performance of the CNT-IE-1 for simultaneous measurement of DA and AA

As the charging current contribution to the background current is a limiting factor in the analytical determination, experiments were carried out using the DPV mode. Using CNT-IE-1 as the working electrode, the analytical experiments were carried out either by varying the AA concentration in the presence of 2.5 μM DA or by varying the DA concentration in the presence of 0.4 mM AA in the pH 5.0 phosphate buffer. Fig. 10 shows DPVs obtained with increasing micromolar concentrations of DA in the presence of 0.4 mM AA and the inset shows the corresponding calibration curve for the DA peak. Fig. 11 shows DPVs obtained for increasing millimolar concentrations of AA in the presence of 2.5 μM DA and the inset shows the corresponding calibration curve for the AA peak. As shown, DA or AA exhibited an excellent DPV response with the signal height of the other component remaining unchanged, thus proving that the responses to DA and AA at the CNT-IE-1 were relatively independent. The current-to-concentration relationship for DA is linear from 0.5 to 10 μM in the presence of 0.4 mM AA, with a correlation coefficient of 0.9994 and a detection limit of 0.1 μM. The linearity of the AA signal ranges from 0.08 to 1.36 mM in the presence of 2.5 μM DA with a correlation coefficient of 0.9998 and a detection limit of 0.02 mM. The current sensitivities were 2.10 μA μM^{-1} and 12.40 μA mM^{-1} for DA and AA, respectively. The reproducibility of measurements using the CNT-IE-1 was 1.8% (n = 5) and 2.2% (n = 5) at 2.5 μM DA and 0.4 mM AA, respectively.

The CNT-IE-1 was prepared repeatedly seven times and used to measure simultaneously 2.5 μM DA and 0.4 mM AA; the RSD was 0.82 and 1.3%, respectively. Using the electrode again after leaving it unused for 2 d, the peak potentials were unchanged and the current signals showed a 1% decrease of the initial response. Practical work required the electrode to be reversible, *i.e.*, it must be possible to use it many times for samples with different concentrations of analyte. Because of the porous structure, DA could easily penetrate into the interfacial layer, which would affect the subsequent measurements. However, it was found that the renewal of the electrode surface was easily accomplished by soaking the modified electrode in PBS and cycling its potential between −0.2 V and 0.6 V, until DA was eliminated with *ca.* 15 scans. No significant changes in peak potentials and currents between new and renewed electrodes were observed.

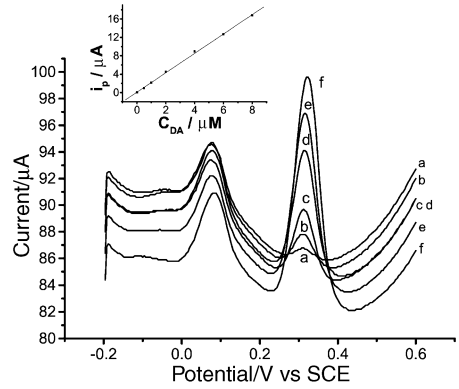

Fig. 10 DPV recordings of DA at CNT-IE-1 in the presence of 0.4 mM AA. DA concentration (μM): (a) 0.5, (b) 1.0, (c) 2.0, (d) 4.0, (e) 6.0 and (f) 8.0. Inset: graph of current *vs.* concentration of DA.

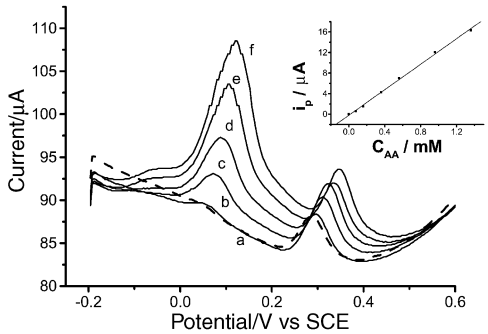

Fig. 11 DPV recordings of AA at CNT-IE-1 in the presence of 2.5 μM DA. AA concentration (mM): (a, dashed line) 0.08, (b) 0.16, (c) 0.36, (d) 0.56, (e) 0.96 and (f) 1.36. Inset: graph of current *vs.* concentration of AA.

Conclusions

Modified electrodes were constructed by casting or intercalating carbon nanotubes on a graphite surface, which resulted in a favorable voltammetric resolution of DA and AA and the anodic potential difference ($\triangle E_{pa}$) was 270 mV in pH 5.0 phosphate buffer. The electrocatalysis of CNT-modified electrodes toward DA and AA was mainly attributed to the stereo porous interfacial layer. The subtle carbon nanotubes provide many active sites, enhancing the sensitivity of DA. The carboxylic acid group attached to carbon nanotubes was an adverse factor for the discrimination of DA from AA. The modified electrodes exhibited an attractive ability to measure DA and AA simultaneously and showed good stability and reproducibility. These attractive features indicate that the carbon nanotube-modified electrode is promising for *in vivo* and *in vitro* measurements of DA and AA.

Acknowledgements

The authors gratefully acknowledge financial support from the National Natural Science Foundation of China (Grant No. 20075015). They thank Dr. Wei Fei for providing carbon nanotube species.

References

1 S. Iijima, *Nature (London)*, 1991, **354**, 56–58.
2 S. Iijima and T. Ichihashi, *Nature (London)*, 1993, **363**, 603–605.
3 S. S. Fan, W. J. Liang, H. Y. Dang, N. Franklin, T. Tombler, M. Chapline and H. J. Dai, *Physica E*, 2000, **8**, 179–183.
4 Z. W. Pan, S. S. Xie and B. H. Chang, *Nature (London)*, 1998, **394**, 631.
5 Q. W. Li, Y. M. Wang and G. A. Luo, *Mater. Sci. Eng. C*, 2000, **11**, 71–74.
6 Q. W. Li and G. A. Luo, *Sens. Actuators, B*, 1999, **59**, 42–49.
7 Q. W. Li and G. A. Luo, *Anal.Chim. Acta*, 2000, **379**, 134–137.
8 J. K. Campbell, L. Sun and R. M. Crooks, *J. Am. Chem. Soc.*, 1999, **121**, 3779–3780.
9 P. J. Britto, K. S. V. Santhanam and P. M. Ajayan, *Bioelectrochem. Bioenerg.*, 1996, **41**, 121–125.
10 J. J. Davis, R. J. Coles and H. A. O. Hill, *J. Electroanal. Chem.*, 1997, **440**, 279–282.
11 J. J. Davis, M. L. H. Green, H. A. O. Hill, Y. C. Leung, P. J. Sadler, J. Sloan, A. V. Xavier and S. C. Tsang, *Inorg. Chim. Acta*, 1998, **272**, 261–266.
12 C. Y. Liu, A. J. Bard, F. Wudl, I. Weitz and J. R. Heath, *Electrochem. Solid State Lett.*, 1999, **2**, 577–578.
13 H. X. Luo, Z. J. Shi, N. Q. Li, Z. N. Gu and Q. K. Zhuang, *Chem. J. Chin. Univ.*,, 2000, **21**, 1372–1374.
14 H. X. Luo, Z. J. Shi, N. Q. Li, Z. N. Gu and Q. K. Zhuang, *Anal. Chem.*, 2001, **73**, 915–920.
15 J. X. Wang, M. X. Li, Z. J. Shi, N. Q. Li and Z. N. Gu, *Electrochim. Acta*, 2001, **47**, 651–657.
16 R. M. Wightman, L. J. May and A. C. Michael, *Anal. Chem.*, 1988, **60**, 769A–779A.
17 C. R. Raj and T. Ohsaka, *J. Electroanal. Chem.*, 2001, **496**, 44–49.
18 J. W. Mo and B. Ogorevc, *Anal. Chem.*, 2001, **73**, 1196–1202.

19 X. L. Wen, Y. H. Jia and Z. L. Liu, *Talanta*, 1999, **50**, 1027–1033.
20 H. Zhao, Y. Z. Zhang and Z. B. Yuan, *Anal. Chim. Acta*, 2001, **441**, 117–122.
21 J. Chen and C. S. Cha, *J. Electroanal. Chem*., 1999, **463**, 93–99.
22 M. D. Rubianes and G. A. Rivas, *Anal. Chim. Acta*, 2001, **440**, 99–108.
23 Y. X. Sun, B. X. Ye, W. M. Zhang and X. Y. Zhou, *Anal. Chim. Acta*, 1998, **363**, 75–80.
24 L. Z. Zheng, S. G. Wu, X. Q. Lin, L. Nie and L. Rui, *Analyst*, 2001, **126**, 736–738.
25 H. Zhao, Y. Z. Zhang and Z. B. Yuan, *Analyst*, 2001, **126**, 358–360.
26 L. Zhang and X. Q. Lin, *Analyst*, 2001, **126**, 367–370.
27 M. Poon and R. L. McCreery, *Anal. Chem*., 1986, **58**, 2745–2750.
28 D. T. Fagan, I. F. Hu and T. Kuwana, *Anal. Chem*., 1985, **57**, 2759.
29 L. Falat and H. Y. Cheng, *Anal. Chem*., 1982, **54**, 2108.
30 T. K. Kawagoe and R. M. Whightman, *Talanta*, 1994, **41**, 865.
31 J. Wang and A. Walcarius, *J. Electroanal. Chem*., 1996, **407**, 183.
32 Ciszewski and G. Milczarek, *Anal. Chem*., 1999, **71**, 1055–1061.
33 K. Miyazaki, G. Matsumoto, M. Yamada, S. Yasui and H. Kaneko, *Electrochim. Acta*, 1999, **44**, 3808–3820.
34 Y. Zhang, Z. Shi and Z. Gu, *Carbon*, 2000, **38**, 2055–2059.
35 Z. J. Jia, Z. Y. Wang and J. Liang, *Carbon*, 1999, **37**, 903–906.
36 J. Liu, A. G. Rinzler and H. J. Dai, *Science*, 1998, **280**, 1253–1256.
37 Peigney, C. H. Laurent, E. Flahaut, R. R. Bacsa and A. Rousset, *Carbon*, 2001, **39**, 507–514.
38 G. N. Kamau, W. S. Willis and J. F. Rusling, *Anal. Chem*., 1985, **57**, 545–551.
39 Q. H. Yang, P. X. Hou, S. Bai, M. Z. Wang and H. M. Cheng, *Chem. Phys. Lett*., 2001, **345**, 18–24.
40 M. S. P. Shaffer; X. Fan and A. H. Windle, *Carbon*, 1998, **36**, 1603–1612.